TU/e EINDHOVEN UNIVERSITY OF TECHNOLOGY

Switching field interval of the sensitive magnetic layer in exchange-biased spin valves

Citation for published version (APA):
Rijks, T. G. S. M., Reneerkens, R. F. O., Coehoorn, R., Kools, J. C. S., Gillies, M. F., Dahlqvist, C., & Jonge, de, W. J. M. (1997). Switching field interval of the sensitive magnetic layer in exchange-biased spin valves. *Journal of Applied Physics*, *82*(7), 3442-3451. https://doi.org/10.1063/1.365660

DOI:
10.1063/1.365660

Document status and date:
Published: 01/01/1997

Document Version:
Publisher's PDF, also known as Version of Record (includes final page, issue and volume numbers)

Please check the document version of this publication:

• A submitted manuscript is the version of the article upon submission and before peer-review. There can be important differences between the submitted version and the official published version of record. People interested in the research are advised to contact the author for the final version of the publication, or visit the DOI to the publisher's website.
• The final author version and the galley proof are versions of the publication after peer review.
• The final published version features the final layout of the paper including the volume, issue and page numbers.

Link to publication

General rights
Copyright and moral rights for the publications made accessible in the public portal are retained by the authors and/or other copyright owners and it is a condition of accessing publications that users recognise and abide by the legal requirements associated with these rights.

• Users may download and print one copy of any publication from the public portal for the purpose of private study or research.
• You may not further distribute the material or use it for any profit-making activity or commercial gain
• You may freely distribute the URL identifying the publication in the public portal.

If the publication is distributed under the terms of Article 25fa of the Dutch Copyright Act, indicated by the "Taverne" license above, please follow below link for the End User Agreement:

www.tue.nl/taverne

Take down policy
If you believe that this document breaches copyright please contact us at:

openaccess@tue.nl

providing details and we will investigate your claim.

Download date: 16. Nov. 2023

Switching field interval of the sensitive magnetic layer in exchange-biased spin valves

Th. G. S. M. Rijks[a),b)] and R. F. O. Reneerkens
Department of Physics, Eindhoven University of Technology, P.O. Box 513, 5600 MB Eindhoven, The Netherlands and Philips Research Laboratories, Prof. Holstlaan 4, 5656 AA Eindhoven, The Netherlands

R. Coehoorn and J. C. S. Kools
Philips Research Laboratories, Prof. Holstlaan 4, 5656 AA Eindhoven, The Netherlands

M. F. Gillies[a)] and J. N. Chapman
Department of Physics and Astronomy, Glasgow University, Glasgow G12 8QQ, United Kingdom

W. J. M. de Jonge
Department of Physics, Eindhoven University of Technology, P.O. Box 513, 5600 MB Eindhoven, The Netherlands

(Received 30 October 1996; accepted 22 June 1997)

The switching field interval, ΔH_s, of Ni–Fe–Co-based thin films and spin-valve layered structures, sputter-deposited on a Ta-buffer layer, was studied. The switching field interval is the field range in which the magnetization reversal of a ferromagnetic layer takes place. In thin films, ΔH_s is determined by the uniaxial anisotropy, induced by growth in a magnetic field. This anisotropy increases with the ferromagnetic layer thickness and saturates at a thickness of 10–25 nm. It also depends on the alloy composition as well as on the choice of the adjacent layers. In exchange-biased spin valves, an additional contribution to ΔH_s was observed, which increases monotonically with increasing interlayer coupling. We explain this in terms of the effect on the magnetization reversal of the sensitive layer due to a simultaneous small, but temporary, magnetization rotation in the exchange-biased layer and lateral variations of the interlayer coupling. In addition, the effect of biquadratic coupling on ΔH_s is discussed. Finally, the thermal stability of ΔH_s is investigated. © *1997 American Institute of Physics.* [S0021-8979(97)01319-4]

I. INTRODUCTION

Since the discovery of the giant magnetoresistance (GMR) effect in magnetic multilayers, there has been considerable effort in applying this effect in magnetoresistive sensors, important for, e.g., high-density recording technology. In this perspective, exchange-biased spin valves of the type $Ni_{80}Fe_{20}/Cu/Ni_{80}Fe_{20}/Fe_{50}Mn_{50}$ prove to be of great interest because of their low-field magnetoresistive behavior.[1,2] $Ni_{80}Fe_{20}$ (permalloy) is sometimes replaced by a Ni–Fe–Co (Ref. 3) or Co–Fe alloy,[4,5] preferably close to a composition such as $Ni_{66}Fe_{16}Co_{18}$ for which the magnetostriction is nearly zero.[6] Especially spin valves with crossed anisotropies of the sensitive and exchange-biased magnetic layers are very favorable for applications, because they exhibit a high sensitivity combined with an extremely low coercivity.[2] Although linearity, coercivity, and several other properties such as noise and high-frequency magnetic behavior also determine the applicability,[7,8] sensitivity is an important issue. The sensitivity is defined as the steepness of the resistance (R) versus field (H) curve

$$s(H_{op}) = \left[\frac{1}{R}\frac{\partial R}{\partial H}\right]_{H=H_{op}}, \tag{1}$$

where H_{op} is the field of operation, i.e., the static field around which the applied field is varied. The sensitivity function is determined by the magnetization-reversal process, and by the current direction, as a result of the superimposed anisotropic magnetoresistance (AMR) effect. For any configuration of field, current, and anisotropy directions, a large sensitivity in the operating point requires a large steepness of the magnetization versus field curve. Equivalently, it requires a small value of the switching field interval, ΔH_s, in which the magnetization reversal of the sensitive layer effectively takes place. A precise definition of ΔH_s will be given below. In an unpatterned spin-valve structure the switching field interval depends on the interplay, between the induced in-plane anisotropy of the magnetic layers, the interlayer coupling, and the exchange-biasing of the pinned magnetic layer. Model treatments of this interplay have been given by Rijks *et al.*[9] (neglecting the induced anisotropy of the sensitive and pinned magnetic layers) and by Parker *et al.*[10] However, so far no systematic experimental study of the switching field interval in exchange-biased spin valves has been carried out.

In this article, we present such a systematic study. As the switching field interval of the sensitive layer in a spin valve is expected to be mainly determined by the induced anisotropy, we first focus on the induced anisotropy of single Ni–Fe–Co thin films, sputter deposited on a Ta buffer layer, with varying film thickness and composition, and for several choices of the adjacent layers. Such an extensive study was motivated by results reported in the literature, showing a marked decrease of the anisotropy field H_K of permalloy thin films with decreasing film thickness, for thicknesses smaller

[a)]Present and permanent address: Philips Research Laboratories, Prof. Holstlaan 4, 5656 AA Eindhoven, The Netherlands.
[b)]Electronic mail: rijks@natlab.research.philips.com

 0021-8979/97/82(7)/3442/10/$10.00 © 1997 American Institute of Physics

Downloaded 31 Aug 2011 to 131.155.151.114. Redistribution subject to AIP license or copyright; see http://jap.aip.org/about/rights_and_permissions

than 40 nm (Ref. 11) or 5 nm (Ref. 12). It is suggested that this is due to island growth in a very early stage of the film deposition. Goto *et al.*[11] proposed a simple model to describe the thickness dependence of H_K in terms of a dead anisotropy layer, i.e., a magnetic layer in which no anisotropy is induced. H_K is then given by

$$H_K = \frac{t_f - t_{d,a}}{t_f} H_{K,\infty}, \tag{2}$$

in which t_f is the film thickness, $t_{d,a}$ is the effective thickness of the dead anisotropy layer, and $H_{K,\infty}$ is the thick-film limit of H_K. This expression describes the data reasonably well when using $t_{d,a} = 10$ nm. In contrast to this, essentially no thickness dependence of H_K is reported in Refs. 13–15. In Ref. 16 no marked thickness dependence of H_K was measured for films sputtered at a pressure of 7 mTorr, whereas in films sputtered at 3 mTorr H_K decreases with decreasing film thickness, below a thickness of 5–10 nm.

Subsequently, we focus on the effect of the interlayer coupling on ΔH_s. We measured ΔH_s of the sensitive layer in a spin valve, as a function of the thickness of the Cu interlayer and the sensitive layer. These measurements show that the switching field interval of the sensitive layer is not solely determined by the induced anisotropy, but that there are additional contributions to ΔH_s, that increase monotonically with increasing interlayer coupling. We will explain this in terms of (i) the effect on the magnetization reversal of the sensitive layer due to a simultaneous small, but temporary, magnetization rotation in the exchange-biased layer and (ii) lateral variations of the interlayer coupling. In addition, the role of biquadratic coupling is discussed.

Finally, we study the change of ΔH_s upon annealing the spin valves. This study was motivated by reports that the induced anisotropy of thin films may change upon annealing in a magnetic field, even at temperatures in the order of 100–200 °C.[17–20] Indeed, we observed that ΔH_s may change dramatically when the spin valves are subjected to elevated temperatures. This is relevant from an applications point of view, since process steps at a temperature of 150–200 °C are very common in the fabrication of magnetoresistive sensing devices. The resulting value of ΔH_s depends strongly on the direction of the magnetic field during the annealing process.

II. EXPERIMENT

Samples were prepared by dc-magnetron sputtering at a base pressure of $5 \cdot 10^{-9}$ Torr and an argon pressure of 5 mTorr (target to substrate distance is 110 mm). Substrates were either 4×12 mm^2 Si(100) single crystals, which had been precleaned by an *ex situ* HF dip, or 12 nm thick Si_3N_4 membranes for transmission electron microscopy (TEM) studies. Basically three types of samples were grown:

(1) 3 nm Ta/t_f F/3 nm Ta, in which F is $Ni_{80}Fe_{20}$, $Ni_{75}Fe_{19}Co_6$, $Ni_{70}Fe_{18}Co_{12}$ or $Ni_{66}Fe_{16}Co_{18}$, and t_f varies from 2 to 50 nm.
(2) 3 nm Ta/t_f F/t_{Cu} Cu/6 nm F/10 nm $Fe_{50}Mn_{50}$/3 nm Ta, where $t_f = 10$ nm and t_{Cu} varies from 1.8 to 2.4 nm for $F = Ni_{80}Fe_{20}$, and $t_f = 8$ nm and t_{Cu} varies from 1.8 to 4.4 nm for $F = Ni_{75}Fe_{19}Co_6$, $Ni_{70}Fe_{18}Co_{12}$, and $Ni_{66}Fe_{16}Co_{18}$.
(3) 3 nm Ta/t_f $Ni_{70}Fe_{18}Co_{12}$/3 nm Cu/6 nm $Ni_{70}Fe_{18}Co_{12}$/10 nm $Fe_{50}Mn_{50}$/3 nm Ta, where t_f varies from 2 to 46 nm.

The Ta buffer layer was used to induce a strong (111) texture, which was confirmed by high angle x-ray diffraction (XRD). The XRD rocking curves show a full width at half-maximum (FWHM) of typically 3°–4°. The deposition rates were about 0.2 nm/s, the layer thicknesses were calibrated using low-angle XRD. During deposition a magnetic field of 15 kA/m was applied, which induces a uniaxial anisotropy in the Ni–Fe–Co layers. In addition, it determines the direction of the exchange anisotropy of the exchange-biased layer in the spin valves, characterized by an exchange-anisotropy field of about 20–25 kA/m. After deposition, the easy direction of the exchange-biased layer was rotated over 90° by heating the sample (under nitrogen flow) to 140 °C, and subsequently cooling down in a magnetic field of 15 kA/m, directed perpendicular to the present easy axis. This yields a spin valve with crossed anisotropies.[2] TEM has shown that the films under investigation are polycrystalline with a columnar grain structure.[21] The average grain size, determined by plan-view TEM, increases monotonically from 5 nm at a film thickness of 5 to about 15 nm at a film thickness of 50 nm.

Magnetization measurements were performed at room temperature using superconducting quantum interference device (SQUID), with the magnetic field directed along the hard axis of the (sensitive) magnetic layer. In a spin valve with crossed anisotropies, this implies that the field is directed along the biasing direction. Lorentz microscopy in the Fresnel mode was performed on samples of type (2) containing $Ni_{80}Fe_{20}$ as the F material, with $t_f = 8$ nm and $t_{Cu} = 2$ and 10 nm.

III. RESULTS AND DISCUSSION

A. Induced anisotropy

The induced-anisotropy field, H_K, has been measured for the films of type (1) as a function of the F-layer thickness, for four different alloy compositions. Figure 1 shows a characteristic magnetization (M) versus field (H) loop of a 3 nm Ta/16.5 nm $Ni_{80}Fe_{20}$/3 nm Ta film, with the magnetic field along the hard axis of the $Ni_{80}Fe_{20}$ layer. This configuration yields a rotation of the magnetization, resulting in a $M(H)$ loop with only very little hysteresis. The anisotropy field is obtained by extrapolating the tangent to the $M(H)$ curve at $M = 0$ to $M = \pm M_s$, as is illustrated in Fig. 1, M_s being the saturation value of the magnetization. The switching field interval ΔH_s equals $2H_K$. In Fig. 2, H_K is displayed as a function of the F-layer thickness t_f. It is shown that for t_f values larger than a certain thickness, H_K is essentially independent of the layer thickness. Below this critical thickness, H_K rapidly decreases with t_f. Our data can be very reasonably described by an expression of the form of Eq. (2). In this expression, however, t_f must be replaced by the effective magnetic layer thickness ($t_f - t_{d,m}$), in which $t_{d,m}$ is

Downloaded 31 Aug 2011 to 131.155.151.114. Redistribution subject to AIP license or copyright; see http://jap.aip.org/about/rights_and_permissions

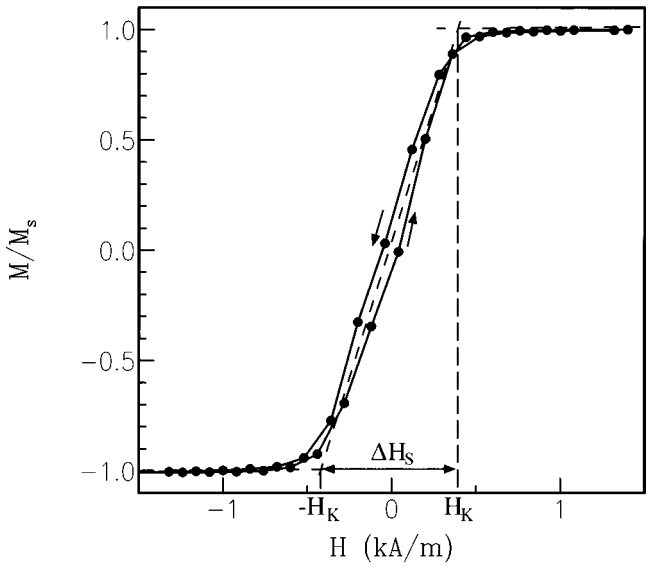

FIG. 1. Magnetization vs field loop of a 3 nm Ta/16.5 nm $Ni_{80}Fe_{20}$/3 nm Ta thin film, with the magnetic field direction along the hard axis. It is demonstrated how the switching field interval ΔH_s is defined.

the effective thickness of the magnetically-dead layer (summed over both interfaces). The values of $t_{d,m}$, tabulated in Table I, are determined from measurements of the saturation magnetic moment as a function of the F-layer thickness. The values of $t_{d,a}$ and $H_{K,\infty}$, determined from fitting the experimental data (solid lines in Fig. 2) are also tabulated in Table I. The parameter $t_{d,a}$ is found to be about 0.6 nm and, within the accuracy, independent of the alloy composition. Although the magnetically-dead layer and the dead anisotropy layer are treated here as independent layers with effective thicknesses, the phenomena of moment and anisotropy reduction are expected to occur simultaneously in the same regions near the interfaces. The origin of the effective layer

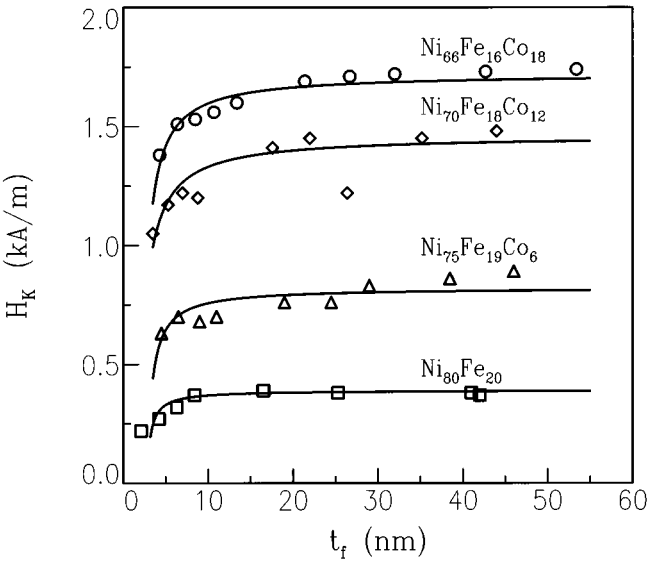

FIG. 2. The anisotropy field H_K as a function of the F-layer thickness t_f, for four different alloy compositions. The lines represent fits using an expression similar to Eq. (2), but taking an effective magnetically-dead layer into account.

TABLE I. The measured values of $t_{d,m}$, and the parameters $t_{d,a}$ and $H_{K,\infty}$ determined by fitting the thickness dependence of the induced anisotropy, using an expression similar to Eq. (2).

Alloy	$t_{d,m}$ (nm)	$t_{d,a}$ (nm)	$H_{K,\infty}$ (kA/m)
$Ni_{80}Fe_{20}$	2.4±1.0	0.4±0.3	0.39±0.01
$Ni_{75}Fe_{19}Co_6$	2.2±1.0	0.6±0.3	0.82±0.02
$Ni_{70}Fe_{18}Co_{12}$	1.0±1.0	0.8±0.3	1.46±0.03
$Ni_{66}Fe_{16}Co_{18}$	1.6±1.0	0.6±0.2	1.72±0.02

thickness with no induced anisotropy, the presence of which results in a thickness dependent H_K, will be discussed now.

When reviewing the results of Refs. 11–16, they can be divided into three categories. First, films that were prepared by rf- or dc-magnetron sputtering at room temperature and high sputter pressure (7–10 mTorr),[14–16] as well as films grown at room temperature by evaporation[13] show no marked thickness dependence of the anisotropy. Second, films that were evaporated at elevated temperatures, show a strong decrease of H_K below a film thickness of about 40 nm.[11] Finally, films prepared at room temperature by ion-beam sputtering (at an argon pressure of 0.1 mTorr)[12] or by low-pressure (3 mTorr) dc-magnetron sputtering[16] show a similar but less pronounced thickness dependence. These results suggest that the thickness dependence of the induced anisotropy is related to the kinetics of the deposition process, i.e., the energy of the atoms arriving at the growing-film surface and the surface mobility of the atoms.

In view of this, three possible explanations for the thickness dependence of H_K can be considered, (i) island growth in a very early stage of the film deposition, as was suggested in Refs. 11 and 12, (ii) interface intermixing, and (iii) a high defect density in the bottom of the magnetic layer. Starting with the first, when island growth is taking place, very small islands could be either paramagnetic, especially when growing at elevated temperatures, or ferromagnetic with a large randomly oriented anisotropy, due to the shape of the islands or due to the specific distribution of the limited number of pairs of Ni and Fe atoms in the island volume.[22] In both cases the magnetization cannot be saturated by the field applied during deposition. Therefore, no anisotropy will be induced in the case of paramagnetism, or no net anisotropy will be induced if the islands are ferromagnetic with a large random anisotropy. After completion of a number of atomic layers with an equivalent thickness of $t_{d,a}$, the film is closed, ferromagnetic, and the random anisotropies have been averaged out to a sufficient extent as a result of the exchange interaction between the previously isolated islands. Now it is possible to saturate the film in the applied field, and an anisotropy will be induced in the subsequently deposited atomic layers. Island growth occurs if the equilibrium growth mechanism is three-dimensional and if the surface diffusion is fast enough, like in the case of low pressure sputtering or when growing at elevated temperatures. In this case one would expect a thickness dependent H_K.[11,12,16] Otherwise, like in the case of room temperature evaporation or high-pressure sputtering, the low surface mobility suppresses the

Downloaded 31 Aug 2011 to 131.155.151.114. Redistribution subject to AIP license or copyright; see http://jap.aip.org/about/rights_and_permissions

TABLE II. Induced anisotropy for various combinations of adjacent layers.

Film	H_K (kA/m)
3 nm Ta/9 nm $Ni_{80}Fe_{20}$/3 nm Ta	0.30
3 nm Ta/9 nm $Ni_{80}Fe_{20}$/3 nm Cu	0.29
3 nm Ta/3 nm Cu/9 nm $Ni_{80}Fe_{20}$/3 nm Ta	0.23
3 nm Ta/3 nm Cu/9 nm $Ni_{80}Fe_{20}$/3 nm Cu	0.22

island formation. In that case, no thickness dependence of H_K is expected.[13–16]

A second possible explanation for the thickness dependence of H_K is interfacial intermixing. When using buffer and cover layers, intermixing at the interfaces will not only influence the magnetic moment, resulting in a magnetically-dead layer, but will possibly also influence the induced anisotropy near the interface. Small amounts of Ta impurities in the magnetic layer could very well disturb the delicate pair ordering process that induces the uniaxial anisotropy. This effect is expected to be significant when the films are prepared by low-pressure sputtering,[12] because in that case the bombardment of energetic atoms causes collisional mixing.

Third, as plan-view TEM shows that the film growth on a Ta-buffer layer starts with a very fine grained structure, a high defect density in the bottom of the magnetic layer could also be responsible for a reduced degree of pair ordering.

In order to investigate the influence of the choice of the adjacent layers, we replaced one or both of the $Ni_{80}Fe_{20}$/Ta interfaces by a $Ni_{80}Fe_{20}$/Cu interface. Being aware of the large influence of Ta as a buffer layer on the film structure, we did not simply replace Ta by Cu but we inserted thin Cu-layers (3 nm) at the $Ni_{80}Fe_{20}$/Ta interfaces. This is also of interest, in view of the fact that our final goal was to study the magnetic behavior of the sensitive layer in a F/Cu/F/$Fe_{50}Mn_{50}$ spin valve. The values of H_K, determined from magnetization measurements, are tabulated in Table II ($t_{NiFe}=9$ nm). It is demonstrated that H_K is significantly reduced with Cu as an adjacent layer, but only when the Cu layer is inserted at the *bottom* $Ni_{80}Fe_{20}$/Ta interface. In Ref. 12 also smaller values of H_K are reported when the $Ni_{80}Fe_{20}$ layer is sandwiched between Cu layers, as compared to Ta. The authors, however, completely replaced the Ta layers, and did not consider the possible influence of changes in the film structure on H_K. The strong reduction of H_K is remarkable as the magnetically-dead layer thickness at a $Ni_{80}Fe_{20}$/Cu interface is only 0.15 nm,[23] which is considerably smaller than the value of 1.2 nm (± 0.5 nm) for a $Ni_{80}Fe_{20}$/Ta interface. Therefore, the influence of an anisotropy-dead layer thickness is expected to be smaller, in view of the larger effective magnetic layer thickness. Although, a certain degree of intermixing is expected to be present at both bottom and top interface, the top interface does not significantly influence H_K. Extensive TEM analyses have shown that thin $Ni_{80}Fe_{20}$ films on Ta develop an almost complete (111) texture, whereas the presence of a thin Cu layer at the bottom $Ni_{80}Fe_{20}$/Ta interface gives rise to a certain fraction of randomly oriented grains.[24,25] Summarizing, this confirms that the details of the initial stages of film growth are of major importance for the development of an induced anisotropy. These details are, however, not yet understood.

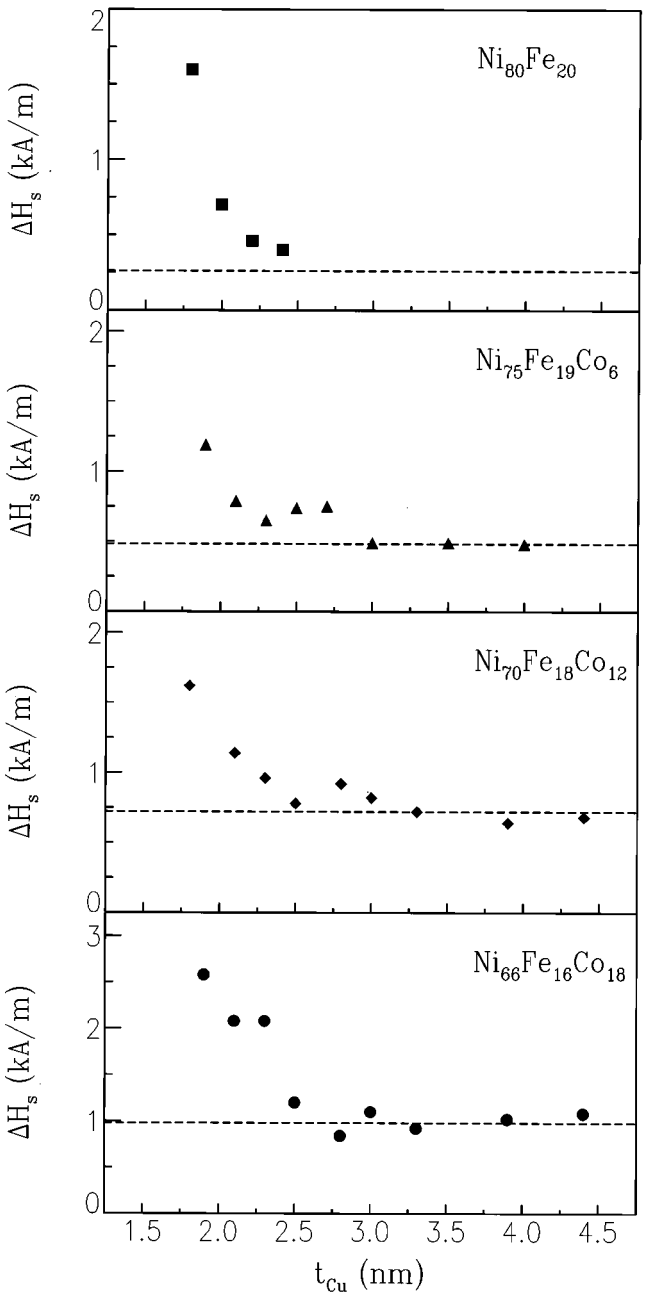

FIG. 3. Switching field interval ΔH_s of Ta/F/Cu/F/$Fe_{50}Mn_{50}$/Ta spin valves as a function of the Cu-layer thickness t_{Cu}, for four different alloy compositions. The dashed lines denote the values of $2H_K$, determined from Ta/F/Cu/Ta films, that are equivalent to spin valves with $t_{Cu}\rightarrow\infty$.

B. Effects of interlayer coupling

Figure 3 shows the switching field interval ΔH_s of the sensitive layer in the spin valves of type (2), as a function of the Cu-interlayer thickness t_{Cu}. For $t_{Cu}>3$ nm, ΔH_s equals the values of $2H_K$ (dashed lines), that were measured on samples of the composition 3 nm Ta/F/3 nm Cu/3 nm Ta, prepared simultaneously with the spin valves. These samples received the same heat treatment as the spin valves. In fact, these samples can be regarded as the sensitive layers of spin

Downloaded 31 Aug 2011 to 131.155.151.114. Redistribution subject to AIP license or copyright; see http://jap.aip.org/about/rights_and_permissions

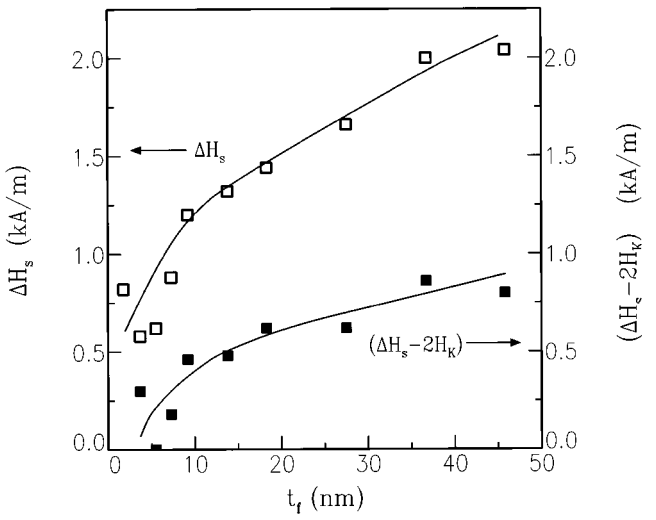

FIG. 4. The switching field interval ΔH_s (open symbols) and the additional contribution to the switching field interval ($\Delta H_s - 2H_K$) (filled symbols), as a function of the thickness t_f of the sensitive layer, for $Ni_{70}Fe_{18}Co_{12}$-based spin valves. The lines are guides to the eye.

valves with an infinitely thick Cu interlayer. It must be remarked that H_K in Fig. 3 is considerably smaller than the values in Fig. 2. It is observed that the heat treatment in a magnetic field perpendicular to the easy axis of the sensitive layer, used to modify the direction of the exchange-biasing field, also results in a decrease of the induced anisotropy in the sensitive layer. This issue will be addressed in more detail in Sec. III C. For $t_{Cu}<3$ nm, ΔH_s increases considerably with decreasing Cu-layer thickness. It is shown in Fig. 4, for $Ni_{70}Fe_{18}Co_{12}$-based spin valves of type (3) with $t_{Cu}=3$ nm, that ΔH_s is dependent on the thickness t_f of the sensitive layer. For comparison, H_K ($=\Delta H_s/2$) of a series of 3 nm Ta/t_f $Ni_{70}Fe_{18}Co_{12}$/3 nm Cu/3 nm Ta thin films was measured as function of the $Ni_{70}Fe_{18}Co_{12}$-layer thickness. Again, these samples received the same heat treatment as the spin valves. Figure 4 shows that $(\Delta H_s - 2H_K)$ is non zero and increases for increasing t_f. So in addition to the induced anisotropy, there is another contribution to the switching field interval that is related to the presence of the second magnetic layer in the spin valve. In this section, we will discuss the extra contribution to ΔH_s in terms of the interactions between the exchange-biased layer and the sensitive layer.

It has been reported by several authors[9,23,26–29] that exchange-biased spin valves, using permalloy or Ni-rich ternary Ni–Fe–Co alloys for the ferromagnetic layers, exhibit a ferromagnetic interlayer coupling. It was shown by Kools[23,29] that the dependence of the coupling constant J_1 on the Cu-layer thickness, for $t_{Cu}>1.5-2$nm, is well described by the Néel model for magnetostatic interlayer coupling, based on the interaction between the dipole fields produced by rough interfaces:[30]

$$J_1=\frac{\pi^2}{\sqrt{2}}\frac{h^2}{\lambda}\mu_0 M_s^2 \exp\left(\frac{-2\pi\sqrt{2}t_{Cu}}{\lambda}\right). \tag{3}$$

Here, λ and h are the lateral length scale and amplitude of the roughness, respectively, and M_s is the saturation magnetization. In this model the roughness is assumed to be two-dimensional and sinusoidal. It is believed that the typical lateral length scale characterizing the roughness is determined by the grain size. Only correlated roughness of the interfaces on either side of the Cu layer is taken into account. The magnetostatic interactions between the top F/Cu interface and the F/Ta interface, as well as between the bottom F/Cu interface and the $F/Fe_{50}Mn_{50}$ interface can be neglected.

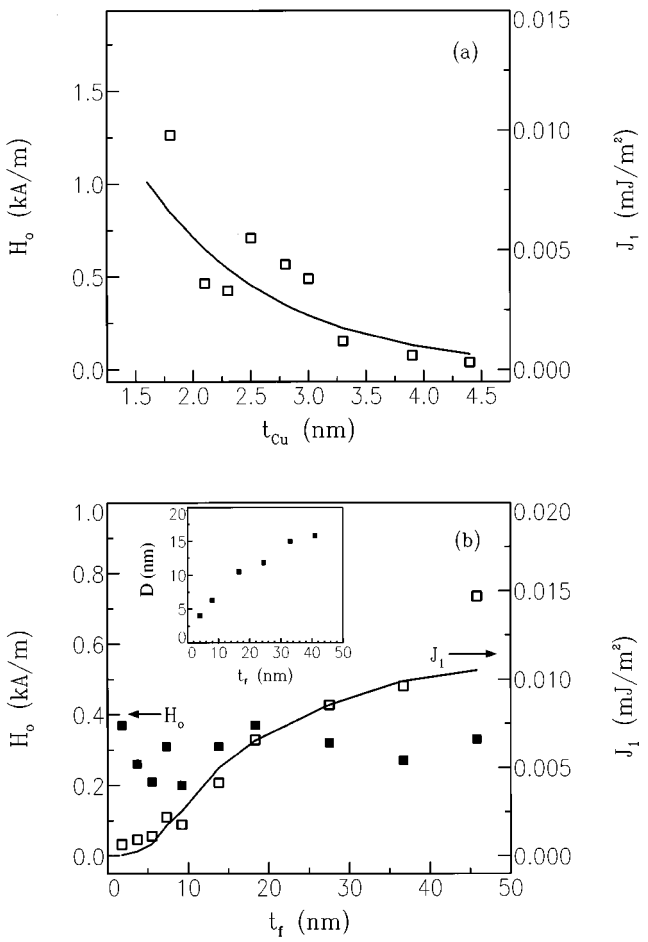

FIG. 5. Offset field H_o (left axis) and bilinear interlayer-coupling constant J_1 (right axis) for $Ni_{70}Fe_{18}Co_{12}$-based spin valves, as a function of the thickness of (a) the Cu interlayer ($t_f=8$ nm) and (b) the sensitive layer ($t_{Cu}=3$ nm). In (b), the filled and open squares represent H_o and J_1, respectively. The lines are fits with the Néel model for magnetostatic interlayer coupling. The inset in (b) shows the average grain size D as a function of the $Ni_{70}Fe_{18}Co_{12}$-layer thickness, as obtained from plan-view TEM measurements.

In exchange-biased spin valves, an interlayer coupling results in a shift from zero field of the $M(H)$ loop of the sensitive layer. This offset field H_o, is defined as the field value at which the total magnetic moment of the sensitive layer is zero. From H_o, the (bilinear) coupling constant J_1 can be calculated, using

$$J_1=\mu_0 M_s H_o t_f, \tag{4}$$

which is valid when the exchange-biasing field $H_{EA} \gg H_o$. It can be shown that Eq. (4) overestimates the value of J_1 when this condition is not fulfilled.[9] As far as our data are concerned, this effect can be neglected. In Fig. 5, the coupling

Downloaded 31 Aug 2011 to 131.155.151.114. Redistribution subject to AIP license or copyright; see http://jap.aip.org/about/rights_and_permissions

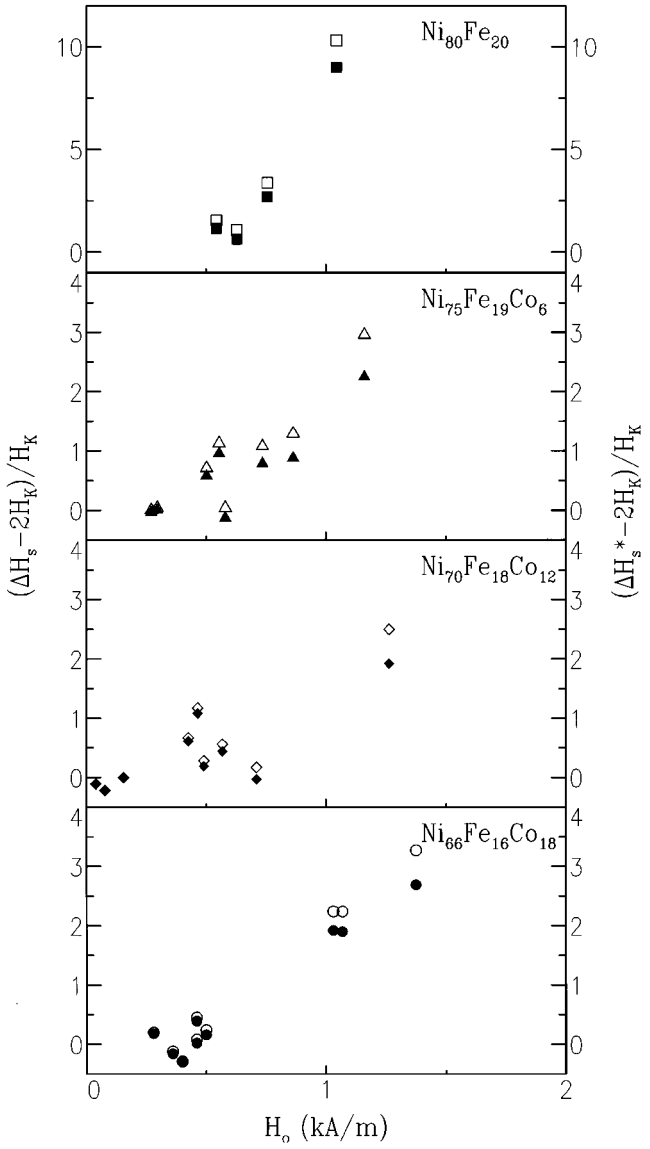

FIG. 6. Additional contribution to the switching field interval $(\Delta H_s - 2H_K)/H_K$ (open symbols) and $(\Delta H_s^\star - 2H_K)/H_K$ (filled symbols) as a function of the offset field H_o, before and after the correction given in Eq. (5), respectively. The data were derived from Fig. 3.

constant J_1 of the $Ni_{70}Fe_{18}Co_{12}$-based spin valves is shown as a function of t_{Cu} [type (2)] and as a function of t_f [type (3)]. The line in Fig. 5(a) represents a fit of the measured data using Eq. (3) and $\mu_0 M_s = 0.97$ T, yielding $\lambda = 10$ nm and $h = 0.25$ nm. These values are consistent with the grain size and roughness amplitude of a 3 nm Ta/8 nm $Ni_{70}Fe_{18}Co_{12}$/3 nm Cu thin film, as measured by plan-view TEM and atomic force microscopy (AFM), respectively. The observation that J_1 also depends on the thickness of the sensitive layer, as shown in Fig. 5(b), may seem somewhat surprising as Eq. (3) does not contain the thickness t_f as an explicit parameter. However, the measured data (squares) are well described by Eq. (3), if for λ the average t_f-dependent grain size D, as measured by plan-view TEM [inset Fig. 5(b)] is used, with constant $h = 0.4$ nm. AFM measurements on 3 nm Ta/t_f $Ni_{70}Fe_{18}Co_{12}$/3 nm Cu thin films showed no evolution of the roughness amplitude with the $Ni_{70}Fe_{18}Co_{12}$-layer thickness. So the increase in coupling strength with increasing thickness of the sensitive layer is entirely ascribed to the evolution of the lateral length scale of the roughness.

In a previous article,[9] we addressed the interplay between the interlayer coupling and the exchange-biasing effect. In that article, we used a minimum-energy model to calculate the magnetization orientation of the magnetic layers in a spin valve, as a function of the interlayer coupling. It was found that the switching field interval increases with the coupling strength, due to the fact that the magnetization reversal of the sensitive layer is accompanied by a small, but temporary, magnetization rotation in the exchange-biased layer. Although, in this model the induced anisotropy was not taken into account, we can use it to make a rough estimate of this effect on ΔH_s. When the coupling energy J_1 is sufficiently small with respect to the exchange-anisotropy energy E_{EA} of the exchange-biased layer, the additional contribution to ΔH_s is estimated by

$$\Delta H = \frac{2j^2}{x} H_{EA} = \frac{2H_o^2}{H_{EA}} \frac{t_f}{t_p}, \tag{5}$$

in which $j = J_1/E_{EA}$, $E_{EA} = \mu_0 M_s H_{EA} t_p$, $x = t_f/t_p$, and J_1 is defined by Eq. (4). In these expressions, t_p and H_{EA} are the thickness of the exchange-biased layer and the exchange-biasing field, respectively. So using $H_{EA} = 20$ kA/m and $t_p = 6$ nm, ΔH can be calculated as a function of H_o, for each series of samples. Correction of ΔH_s for this effect yields $\Delta H_s^\star \equiv \Delta H_s - \Delta H$. In Fig. 6 $(\Delta H_s - 2H_K)/H_K$ (open symbols) and $(\Delta H_s^\star - 2H_K)/H_K$ (filled symbols), derived from the data in Fig. 3, are displayed as a function of H_o. Figure 6 shows that there is still a contribution $(\Delta H_s^\star - 2H_K)$ to the switching field interval that remains unexplained. The fair correlation between $(\Delta H_s^\star - 2H_K)/H_K$ and H_o provides support for the point of view, that also this additional contribution to the switching field interval is closely related to the interlayer coupling. We can use Eq. (5) also to correct the values of ΔH_s for varying t_f (Fig. 4). When inserting the values of H_o and t_f from Fig. 5(b), ΔH is found to increase from ~ 0.004 kA/m for $t_f = 4$ nm, to approximately 0.08 kA/m for $t_f = 46$ nm. This effect is almost an order of magnitude smaller than the measured values of $(\Delta H_s - 2H_K)$. It must be remarked that the increasing Zeeman energy of the sensitive layer when t_f increases favors a reduction of the switching field interval and therefore counteracts the effect of the coupling on ΔH_s. In Fig. 7 $(\Delta H_s - 2H_K)/H_K$ (open symbols) and $(\Delta H_s^\star - 2H_K)/H_K$ (filled symbols), derived from the data in Fig. 4, are displayed as a function of $\mu_0 M_s H_o t_f$. In order to explain the additional contribution to ΔH_s, we will now consider the effect of lateral variations of the bilinear coupling. In addition, the role of biquadratic coupling is discussed.

The general form of a hard axis $M(H)$ curve with an offset field H_o is given by

Downloaded 31 Aug 2011 to 131.155.151.114. Redistribution subject to AIP license or copyright; see http://jap.aip.org/about/rights_and_permissions

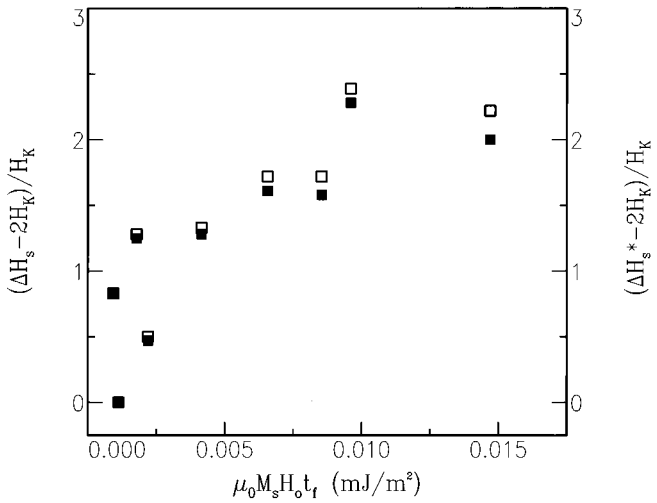

FIG. 7. Additional contribution to the switching field interval $(\Delta H_s - 2H_K)/H_K$ (open symbols) and $(\Delta H_s^* - 2H_K)$ (filled symbols), for $Ni_{70}Fe_{18}Co_{12}$-based spin valves, as a function of $\mu_0 M_s H_o t_f$, before and after the correction given in Eq. (5), respectively. The data were derived from Fig. 4.

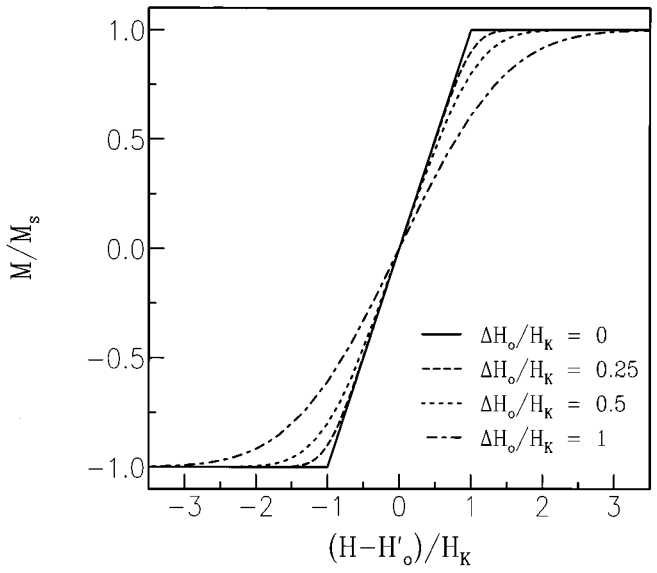

FIG. 8. Calculated $M(H)$ curves as a function of $(H-H'_o)/H_K$, for various values of $\Delta H_o/H_K$.

$$M(H) = -M_s, \quad \text{if } H + H_o < -H_K,$$

$$M(H) = \left(\frac{H+H_o}{H_K}\right)\cdot M_s, \quad \text{if } -H_K \leqslant H + H_o \leqslant H_K, \tag{6}$$

$$M(H) = M_s, \quad \text{if } H + H_o > H_K.$$

A laterally varying coupling strength results in a distribution of offset fields, when the variations take place on a length scale large enough to allow independent switching of the magnetization in different regions. To demonstrate the effect of this on the $M(H)$ curve, let us consider the specific case of a Gauss distribution of H_o values around an average value H'_o, with a standard deviation ΔH_o. Equation (6) is then replaced by

$$M(H) = \int_{-\infty}^{-H_K - H} dH_o(-M_s)\cdot p(H_o) + \int_{-H_K-H}^{H_K-H} dH_o\left(\frac{H+H_o}{H_K}\right)\cdot M_s \cdot p(H_o) + \int_{H_K-H}^{\infty} dH_o M_s \cdot p(H_o), \tag{7}$$

in which the distribution function $p(H_o)$ is given by

$$p(H_o) = \frac{1}{\Delta H_o \sqrt{2\pi}} \exp\left[-\frac{1}{2}\left(\frac{H_o - H'_o}{\Delta H_o}\right)^2\right]. \tag{8}$$

The calculated $M(H)$ curves as a function of $(H-H'_o)/H_K$ are displayed in Fig. 8, for various values of $\Delta H_o/H_K$. It is shown that a distribution of H_o values has two effects on the $M(H)$ curve: it leads to a rounding of the $M(H)$ curve and to an enhancement of ΔH_s. The switching field interval can be calculated from Eq. (7) using

$$\Delta H_s = \frac{2M_s}{\left[\frac{\partial M}{\partial H}\right]_{H=H'_o}} = \frac{2H_K}{\text{erf}\left(\frac{H_K}{\Delta H_o \sqrt{2}}\right)}, \tag{9}$$

in which erf is the error function defined by

$$\text{erf}(x) = \frac{2}{\sqrt{\pi}}\int_0^x dt\ \exp(-t^2). \tag{10}$$

Figure 9 shows the (normalized) contribution to the switching field interval as a function of $\Delta H_o/H_K$. Within this model $(\Delta H_s - 2H_K)/H_K$ is negligible for $\Delta H_o < 0.3H_K$ and becomes appreciable for larger values of ΔH_o. This is basically the same behavior as was measured as a function of H_o

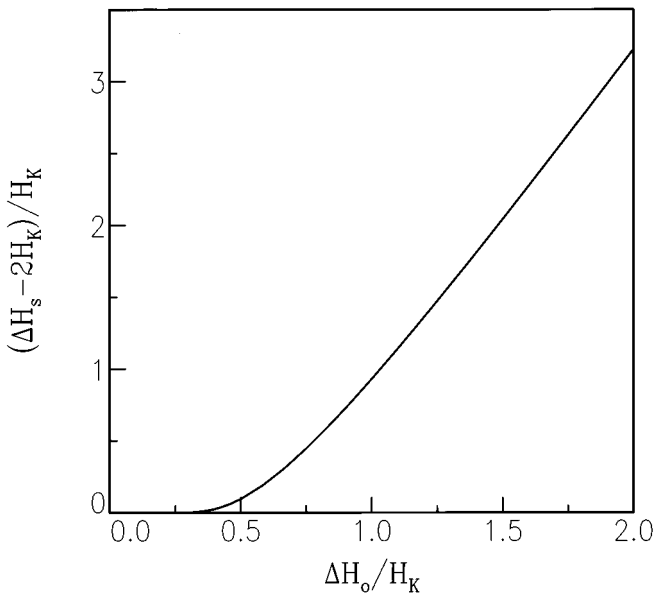

FIG. 9. Normalized contribution to the switching field interval $(\Delta H_s - 2H_K)/H_K$ as a function of $\Delta H_o/H_K$.

Downloaded 31 Aug 2011 to 131.155.151.114. Redistribution subject to AIP license or copyright; see http://jap.aip.org/about/rights_and_permissions

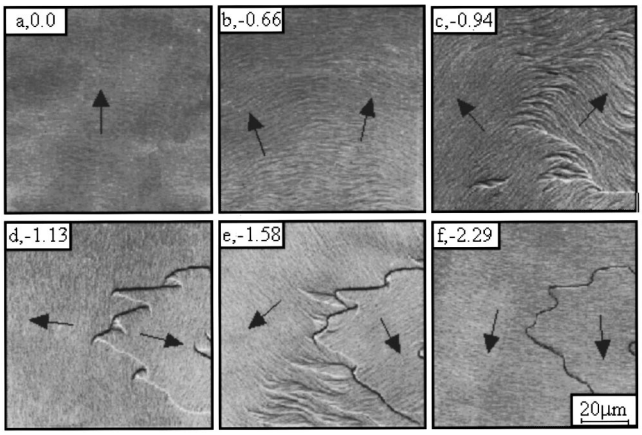

FIG. 10. Sequence of Lorentz micrographs, obtained in the Fresnel imaging mode, of a $Ni_{80}Fe_{20}$-based spin valve with a Cu-layer thickness of 2 nm. The magnetic field, indicated in kA/m, is directed perpendicular to the easy axis of the sensitive layer (along the vertical axis of the micrographs). The arrows indicate the directions of the magnetization.

(Fig. 6), indicating that ΔH_o increases with H_o when the thickness of the Cu interlayer decreases. Although, the structural origin of the lateral variations in coupling strength is expected to remain unchanged, the effect of these variations becomes more distinct when t_{Cu} is decreased. The dependence of $(\Delta H_s - 2H_K)/H_K$ on the thickness of the sensitive layer (Fig. 7) is ascribed to changes in the structural origin of the lateral variations in the coupling strength. The changes in the film structure as a function of t_f were discussed earlier.

Direct evidence for the occurrence of a laterally inhomogeneous switching behavior is presented in Figs. 10 and 11. These figures display sequences of Lorentz micrographs, obtained in the Fresnel imaging mode, showing the magnetization reversal of the sensitive layer of 3.5 nm Ta/8 nm $Ni_{80}Fe_{20}/t_{Cu}$ Cu/6 nm $Ni_{80}Fe_{20}$/10 nm $Fe_{50}Mn_{50}$/5nm Ta spin valves with a Cu-layer thickness of 2 nm (Fig. 10) and 10 nm (Fig. 11). The values of the magnetic field, directed perpendicular to the easy axis of the sensitive layer, are indicated in kA/m. Although some domain walls can be observed, both

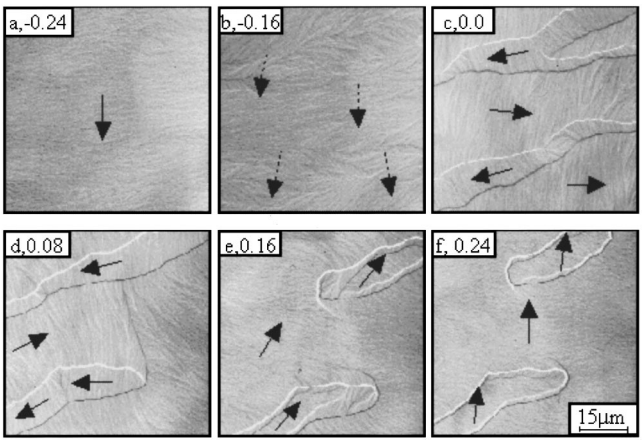

FIG. 11. Sequence of Lorentz micrographs, obtained in the Fresnel imaging mode, of a $Ni_{80}Fe_{20}$-based spin valve with a Cu-layer thickness of 10 nm. The magnetic field, indicated in kA/m, is directed perpendicular to the easy axis of the sensitive layer (along the vertical axis of the micrographs). The arrows indicate the directions of the magnetization.

magnetization reversals show a coherent rotation over large fractions of the sample, as evidenced by the orientation of the magnetization ripple. Magnetization ripple, which is a local dispersion in the direction of the magnetization, is imaged in the Fresnel mode of Lorentz microscopy as a pattern of low contrast black and white lines perpendicular to the average magnetization.

For the strongly-coupled spin valve ($t_{Cu}=2$ nm), one observes that the reversal process is initiated at fields around -0.7 kA/m, while it requires fields as large as -2.3 kA/m to complete the reversal process. This yields a value of ΔH_s of 1.6 kA/m, which is consistent with the data in Fig. 3. The weakly-coupled spin valves displays a rotation of the magnetization that is completed in a smaller field interval, i.e., between $H=0.15$ kA/m and $H=-0.2$ kA/m. A more striking difference between Figs. 10 and 11 is found in the degree of lateral variations. While a large fraction of the free layer reversal of the weakly-coupled spin valve is made up of rotation, some domain structures are seen to form. As deduced from the ripple pattern within these domains, which is essentially parallel within each domain, one observes no significant dispersion of the magnetization direction. For the strongly-coupled spin valves one observes, although an exact quantification the ripple intensity is difficult, that the ripple pattern at the onset of reversal is much more pronounced. In addition, it is observed that the field at which the maximum ripple intensity occurs is varying over the area of investigation [compare, e.g., Figs. 10(e) and 11(e)].

Both effects can be attributed to more pronounced lateral variations of the coupling strength in the strongly-coupled spin valve. As the interlayer coupling is the only parameter that is different for the spin valves of Figs. 10 and 11, any differences in the phenomena observed must be due to coupling-related effects. As was discussed earlier, the mechanism responsible for the interlayer coupling is associated with the magnetostatic effects of topological features, and it is reasonable to assume that lateral variations of the density of these topological features result in an inhomogeneous coupling *constant*. The exchange and magnetostatic interactions in the ferromagnetic layers will result in an averaging of the coupling *field* over areas determined by the exchange length, giving rise to a ripple pattern caused by this laterally varying coupling. More pronounced lateral variations of the coupling strength lead to a more pronounced ripple pattern at the onset of magnetization reversal, which is indeed observed. If the degree of the variations is such that the local coupling field after this averaging is still laterally dependent, areas switching at different offset fields will be observed (Fig. 10) as was assumed in Eqs. (7) and (8).

In an earlier study of coupling effects in exchange-biased spin valves, we already found indications for an inhomogeneous switching behavior of the sensitive layer from an increased rounding of the (usually square) resistance versus field loops, when the Cu-layer thickness is decreased.[9]

Now, we will consider the possible effect of biquadratic coupling on the switching field interval. In addition to the magnetostatic bilinear coupling due to correlated roughness, with a coupling energy $E_1 = J_1 \cos \vartheta$, Demokritov *et al.* have shown that uncorrelated roughness leads to a magneto-

Downloaded 31 Aug 2011 to 131.155.151.114. Redistribution subject to AIP license or copyright; see http://jap.aip.org/about/rights_and_permissions

static coupling-energy term of the form $E_2 = J_2 \cos^2 \vartheta$. Here, ϑ is the angle between the magnetization directions of adjacent layers. This is called biquadratic coupling or 90-degree coupling,[31] and it has been observed in epitaxially grown Fe/Au/Fe sandwiches.[32] In spin valves with a configuration of crossed anisotropies, the biquadratic coupling-energy term is mathematically identical to the uniaxial anisotropy energy, and therefore, enhances the effective uniaxial anisotropy of the sensitive layer. The effective anisotropy field is then given by

$$H_{\mathrm{K,eff}} = H_{\mathrm{K}} + \frac{J_2}{t_{\mathrm{f}}} \frac{1}{\frac{1}{2}\mu_0 M_{\mathrm{s}}}. \tag{11}$$

In Ref. 31, an expression for J_2 is derived for a specific case of uncorrelated (one-dimensional) roughness, viz., with one flat and one rough interface:

$$J_2 = \frac{\mu_0^2 M_{\mathrm{s}}^4 h^2 \lambda}{4\pi^3 A'} \exp\left(\frac{-4\pi t_{\mathrm{Cu}}}{\lambda}\right)\left[1 - \exp\left(\frac{-8\pi t_{\mathrm{f}}}{\lambda}\right)\right]. \tag{12}$$

In Eq. (12), $A' \approx A$, the exchange stiffness ($A \approx 10^{-11}$ J/m). When inserting typical parameter values as used above for the calculation of bilinear Néel-type coupling, viz. $\mu_0 M_{\mathrm{s}} = 0.97$ T ($M_{\mathrm{s}} = 776$ kA/m), $h = 0.25$ nm, $t_{\mathrm{Cu}} = 2$ nm, $t_{\mathrm{f}} = 8$nm, and $\lambda = 10$ nm, Eq. (12) yields $J_2 = 2.3 \cdot 10^{-8}$ J/m^2. The second term of Eq. (11) then becomes 5.9 A/m, which is 2–3 orders of magnitude smaller than the typical values of H_{K}. Therefore, we conclude that a possible contribution of biquadratic coupling to the switching field interval can be neglected here.

C. Thermal stability of the switching field interval

The thermal stability of the switching field interval ΔH_{s} was investigated for a number of identical $Ni_{80}Fe_{20}$ spin valves, consisting of 3 nm Ta/8 nm $Ni_{80}Fe_{20}$/2.5 nm Cu/6 nm $Ni_{80}Fe_{20}$/10 nm $Fe_{50}Mn_{50}$/3 nm Ta. Here, it is important to stress that after deposition we have a configuration of *parallel* anisotropies. This study is motivated by the fact that a heat treatment in a magnetic field is required to create the configuration of *crossed* anisotropies (see Sec. II). In the fabrication of a magnetoresistive sensing device there are also other process steps at elevated temperatures. Here, we are especially interested in the influence of the direction of a magnetic field during the heat treatment. In our experiments, the samples were heated to 140 °C and maintained at this temperature for a certain period of time, different for each sample. A set of four samples was annealed during $(t_{\mathrm{A}} - 5)$ minutes in a magnetic field (of about 15 kA/m) aligned parallel to the easy axes of the sensitive and exchange-biased layer (=field direction during growth), followed by 5 min of annealing and subsequent cooling in a field perpendicular to the easy axes, in order to achieve a configuration of crossed anisotropies. The last step is necessary in order to be able to measure a hard axis $M(H)$ loop of the sensitive layer and determine ΔH_{s}. Another set of five samples was annealed during t_{A} min, and subsequently cooled, in a field perpendicular to the easy axes, therefore, automatically yielding a configuration of crossed anisotropies. After cooling down the samples, ΔH_{s} was measured at room temperature. The results for both sets of samples are plotted in Fig. 12, as a function of the total annealing time t_{A}. The results are compared to a sample in which the anisotropies were crossed during sputtering, by mechanically rotating the field direction between the deposition of both $Ni_{80}Fe_{20}$ layers. So this sample was not subjected to any heat treatment and ΔH_{s} equals 0.41 kA/m (filled square). It is clearly demonstrated in Fig. 12 that only 5 min of annealing in a perpendicular field already leads to a significant reduction of ΔH_{s}, with respect to the sample that did not receive any heat treatment. Further, perpendicular annealing reduces ΔH_{s} even more to 0.24 kA/m (open triangles), whereas parallel annealing increases the ΔH_{s} considerably up to 0.52 kA/m (filled triangles). One sample was annealed for 4 h in the absence of a magnetic field followed by 5 min of perpendicular annealing, which resulted in a value of ΔH_{s} of 0.46 kA/m (+ symbol).

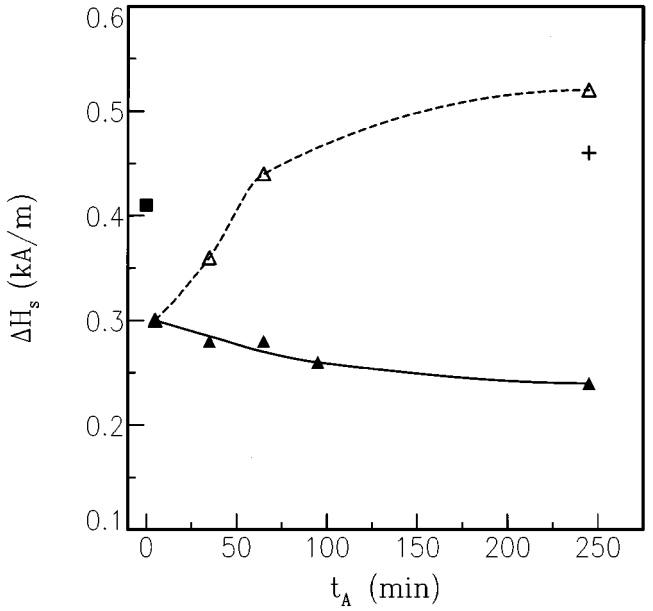

FIG. 12. Switching field interval ΔH_{s} vs the total annealing time t_{A} with the magnetic field parallel (open triangles) and perpendicular (filled triangles) to the easy axes. The lines are guides to the eye. The filled square represents a sample that was not subjected to any heat treatment, the cross represents a sample that was annealed without the presence of a magnetic field.

These changes of the switching field interval upon annealing, that have also been observed in $Ni_{80}Fe_{20}$ thin films,[33] are attributed to changes in the induced anisotropy due to atomic diffusion. During the heat treatment atomic diffusion causes the formation of atom pairs with the pair axis along a direction defined by the local magnetization direction, the so-called directional ordering, which is believed to be the origin of the induced anisotropy.[34,35] The phenomenon that the induced anisotropy changes upon annealing in a magnetic field is well known (see, e.g., Refs. 17–20). Depending on the direction of the field during heating, this will either enhance (parallel) or reduce (perpendicular) the anisotropy created by directional ordering during deposition in a magnetic field. At such a low temperature, the diffusion process involved is expected to be defect diffusion that takes place in the vicinity of grain boundaries,

Downloaded 31 Aug 2011 to 131.155.151.114. Redistribution subject to AIP license or copyright; see http://jap.aip.org/about/rights_and_permissions

where usually a high atom mobility exists.[36] Grain boundaries are abundantly present in our polycrystalline films. The interlayer coupling was found to be unaffected by the heat treatment, which makes it very unlikely that the change in switching field interval is due to a change in the lateral variations of the coupling field. Moreover, such a mechanism could not explain the dependence on the field direction. The sample that was annealed in the absence of a magnetic field also shows an increased ΔH_s, comparable to the samples that were subjected to 4 h of parallel heating followed by 5 min of perpendicular annealing. This is due to the spontaneous alignment of the sensitive-layer magnetization along the already present easy axis. In this experiment, the switching field interval obtained is of course very sensitive to stray-field components perpendicular to the easy axis, if they are significantly large with respect to the anisotropy field before heat treatment of 0.2 kA/m. We want to point out here that heat treatment can, on the one hand, be an important tool to control the contribution of the induced anisotropy to the switching field interval of the sensitive layer, and consequently the sensitivity and the noise of a magnetoresistive sensor.[37] On the other hand, one should be careful with subjecting the spin valves to elevated temperatures without proper control of the magnetic field direction, as stray fields could influence the induced anisotropy, and therefore, the switching field interval in an unpredictable manner.

IV. CONCLUSIONS

We have studied the switching field interval ΔH_s of Ni–Fe and Ni–Fe–Co-based thin films and spin valves, sputter-deposited on a Ta-buffer layer. In thin films, ΔH_s is determined by the induced anisotropy, that is found to depend on the ferromagnetic layer thickness, as well as on the choice of the adjacent layers. This effect may be related to the growth mode of the first few atomic layers. In spin valves, an additional contribution to ΔH_s was discovered, that increases monotonically with increasing interlayer coupling. We explain this in terms of (i) the effect on the magnetization reversal of the sensitive layer due to a simultaneous small, but temporary, magnetization rotation in the exchange-biased layer, and (ii) lateral variations of the interlayer coupling. The latter is corroborated by Lorentz-microscopy observations and is found to be dominant. We also considered a possible contribution from magnetostatic biquadratic coupling. This can, however, be neglected. Finally, we have demonstrated that ΔH_s is very sensitive to heat treatments. Annealing at a temperature of about 140 °C results in an increase or decrease of the induced anisotropy, depending on the direction of the magnetic field during the anneal treatment.

ACKNOWLEDGMENTS

The authors wish to thank A. E. M. De Veirman for the TEM analysis, H. A. G. Nulens for the AFM measurements. This research is part of the European Union ESPRIT3 Basic Research Project, Study of Magnetic Multilayers for Magnetoresistive Sensors (SmMmS) and was supported by the Technology Foundation (STW).

[1] B. Dieny, V. S. Speriosu, S. Metin, S. S. P. Parkin, B. A. Gurney, P. Baumgart, and D. R. Wilhoit, J. Appl. Phys. **69**, 4774 (1991).
[2] Th. G. S. M. Rijks, W. J. M. de Jonge, W. Folkerts, J. C. S. Kools, and R. Coehoorn, Appl. Phys. Lett. **65**, 916 (1994).
[3] W. Folkerts, J. C. S. Kools, M. C. de Nooijer, J. J. M. Ruigrok, L. Postma, K.-M. H. Lenssen, G. H. J. Somers, and R. Coehoorn, IEEE Trans. Magn. **31**, 2591 (1995).
[4] H. Yoda, H. Iwasaki, A. Tsutai, and M. Sahashi, Digests of the INTERMAG'96 (Seattle, Washington, 1996), AA-01.
[5] H. Kanai, K. Yamada, K. Aoshima, Y. Ohtsuka, J. Kane, M. Kanamine, J. Toda, and Y. Mizoshita, see Ref. 4, AA-O2.
[6] C. H. Wilts and F. B. Humphrey, J. Appl. Phys. **39**, 1191 (1968).
[7] K.-M. H. Lenssen, H. W. van Kesteren, Th. G. S. M. Rijks, J. C. S. Kools, M. C. de Nooijer, and W. Folkerts, Sensors and Actuators A (submitted).
[8] J. C. S. Kools, J. J. M. Ruigrok, M. C. de Nooijer, and W. Folkerts, IEEE Trans. Magn. (submitted).
[9] Th. G. S. M. Rijks, R. Coehoorn, J. T. F. Daemen, and W. J. M. de Jonge, J. Appl. Phys. **76**, 1092 (1994).
[10] M. R. Parker, H. Fujiwara, and S. Hossain, IEEE Trans. Magn. **31**, 2618 (1995).
[11] M. Goto, H. Tange, and T. Kamimori, J. Magn. Magn. Mater. **62**, 251 (1986).
[12] M. Ueno and S. Tanoue, J. Vac. Sci. Technol. A **13**, 2194 (1995).
[13] M. Takahashi, J. Appl. Phys. Suppl. to **33**, 1101 (1962).
[14] K. Solt, Thin Solid Films **125**, 251 (1985).
[15] R. M. Valletta, G. Guthmiller, and G. Gorman, J. Vac. Sci. Technol. A **9**, 2093 (1991).
[16] A. Tsoukatos, S. Gupta, and Y. K. Kim, J. Appl. Phys. **79**, 5446 (1996).
[17] G. Kneer and W. Zinn, Phys. Status Solidi **17**, 323 (1966).
[18] D. O. Smith, G. P. Weiss, and K. J. Harte, J. Appl. Phys. **37**, 1464 (1966).
[19] T. Fujii, S. Uchiyama, M. Masuda, and Y. Sakaki, IEEE Trans. Magn. **MAG-4**, 515 (1968).
[20] S. J. Horowitz and M. L. Rudee, Phys. Status Solidi A **5**, 427 (1971).
[21] P. Galtier, R. Jerome, and T. Valet, in *Polycrystalline Thin Films, Structure, Texture, Properties, and Applications*, edited by K. Barmak, M. A. Parker, J. A. Floro, R. Sinclair, and D. A. Smith (Materials Research Society, Pittsburgh, Pennsylvania, 1994), p. 417.
[22] R. Coehoorn, R. F. O. Reneerkens, and Th. G. S. M. Rijks (unpublished).
[23] J. C. S. Kools, J. Appl. Phys. **77**, 2993 (1995).
[24] A. E. M. De Veirman, J. J. T. M. Donkers, and K.-M. H. Lenssen (unpublished).
[25] K.-M. H. Lenssen, A. E. M. De Veirman, and J. J. T. M. Donkers, J. Appl. Phys. **81**, 4915 (1997).
[26] H. S. Joo and H. A. Atwater, IEEE Trans. Magn. **31**, 3946 (1995).
[27] K. Nishioka, S. Gangopadhyay, H. Fujiwara, and M. Parker, IEEE Trans. Magn. **31**, 3949 (1995).
[28] K. Hoshino, S. Noguchi, R. Nakatani, H. Hoshiya, and Y. Sugita, Jpn. J. Appl. Phys., Part 1 **33**, 1327 (1994).
[29] J. C. S. Kools, Th. G. S. M. Rijks, A. E. M. De Veirman, and R. Coehoorn, IEEE Trans. Magn. **31**, 3918 (1995).
[30] L. Néel, Comptes Rendus **255**, 1676 (1962).
[31] S. Demokritov, E. Tsymbal, P. Grünberg, W. Zinn, and I. K. Schuller, Phys. Rev. B **49**, 720 (1994).
[32] U. Rücker, S. Demokritov, E. Tsymbal, P. Grünberg, and W. Zinn, J. Appl. Phys. **78**, 387 (1995).
[33] Th. G. S. M. Rijks (unpublished).
[34] L. Néel, J. Phys. Radium **15**, 225 (1954).
[35] S. Taniguchi, Sci. Rep. Res. Inst. Tohoku Univ. A **7**, 269 (1955).
[36] M. Roth, J. Appl. Phys. **41**, 1286 (1970).
[37] T. Yeh and W. F. Witcraft, IEEE Trans. Magn. **31**, 3131 (1995).

Downloaded 31 Aug 2011 to 131.155.151.114. Redistribution subject to AIP license or copyright; see http://jap.aip.org/about/rights_and_permissions